A Pattern Analysis-based Segmentation to Localize Early and Late Blight Disease Lesions in Digital Images of Plant Leaves

*Aliyu Muhammad Abdu
School of Electrical Engineering
University Technology Malaysia,
81310 Johor, Malaysia
Email: aliyu104@yahoo.com

Musa Mohd Mokji
School of Electrical Engineering
University Technology Malaysia,
81310 Johor, Malaysia
musamm@utm.my

Usman Ullah Sheikh
School of Electrical Engineering
University Technology Malaysia,
81310 Johor, Malaysia
usman@fke.utm.my

***Abstract*— This study reports a disease symptom classification algorithm using a proposed pattern recognition approach to individually localize early and late blight visual disease symptoms. The algorithm uses the pathological analogy hierarchy of the diseases to produce a novel homogeneous pattern localization, more informative to extract features that would be utilized for a machine learning system to classify the two diseases in digital photographs of vegetable plants. One of the most significant advantages of the proposed pattern analysis is localizing symptomatic and necrotic regions based on pathological disease analogy using soft computing, with which the pattern of each disease manifestation along the leaf surface can be tracked and quantified for characterization. In the 1st phase of the experiment, individual symptomatic (R_S), necrotic (R_N), and blurred (R_B, in-between healthy and symptomatic) regions were identified, segmented, and quantified. The 2nd phase focuses on the extraction of pattern features for classification and severity estimation with a machine learning classifier. The obtained results are encouraging, successfully localizing and quantifying individual disease lesions. This also indicates the enhanced applicability of the proposed approach discriminating the two diseases based on their dissimilarity. It is also envisaged that the algorithm can be extended to other plant disease symptoms. Moreover, it provides opportunities for early identification and detection of subtle changes in plant growth, disease stage, and severity estimation to assisting crop diagnostics in precision agriculture.**

Keywords*— *Pattern analysis, Computer vision, Segmentation, Plant disease lesion, Plant disease detection

I. INTRODUCTION

A. Background

Phenotyping, the basis used for segmentation, is the physical and biological characteristics of an organism as determined by its genetic interaction with the environment [1]. The use of image analysis tools for the measure of plant disease phenotyping at a scale of the leaf did not receive much attention until the 1970s and 80s when desktop computers, image analysis software programs and relatively inexpensive digital cameras emerged [2]. By then, expert pathologist actively started comparing assessment methods quantitatively. Earlier Pioneers on application of image processing in plant pathology were those who considered its applicability to disease assessment such as Nelson *et al.* described using texture analysis system in calculating area of fungal infection on leaves and distribution of lesions [3], and Blanchette who used image analyzer system and demonstrated its technological approach to measure in severity of wood decay [4]. Such early methodologies pioneered future studies featured to precision agriculture and demonstrated the capacity of image analysis to measure disease severity such as that of Lindow and Webb (1983) and Lindow (1983) [5, 6]. Image processing techniques embedded with trained machine learning classifiers are now mostly the machinery that classifies diseases in the digital images that usually packed in image dataset or individual captured photos. It then followed that over the last decade, plant disease detection using machine learning had gained tremendous momentum, an active area of research in precision agriculture [1, 2, 8, 11].

Numerous researches have been reported in the literature that employed different aspects of machine learning (ML) methods for plant disease detection [7-11], the majority of which focused on the plant leaves. The entire ML process involves four stages preprocessing called segmentation, feature extraction, and classification [1, 8, 10, 12]. Segmentation and subsequent feature extraction are the key steps that determine the applicability of every machine learning model which detection and classification are generally based on [1, 8]. The features would be a collection of redundant patterns of properties that sufficiently portray the quantifiable detail of the target region [1]. Each feature would then quantifiably interpret the disease pattern and in general sense, portray the similarity or not between the localized pixels. A common practice is to perform segmentation of disease symptom regions before features extraction by first removing or masking the background leaving only the leaf, then later removing healthy green pixel regions thereby creating a region of interest (ROI) [12]. This step, however, is not necessary when using a deep learning framework. The now popular Convolution Neural Network-based (CNN) methods can automatically extract the features directly from the input images and unlike crafted features explicitly bypassing the feature extraction steps [1]. Commonly associated features are texture, color, and shape [1, 7, 13], categorized as handcrafted or custom features-based employed with statistical classifiers such as Support Vector Machine (SVM) and Naïve Bayes and convolution neural network (CNN)-based approaches employed by deep learning framework [1]. This work focused on custom-based features were suggested as preferable to segmentation of plant parts in aerial photographs in the visible spectrum.

The absolute majority of the existing methods for disease classification perform disease lesion segmentation simply on the perception that tissue with purely green color is healthy and discolored (another color deviating from purely green) is diseased [1, 8, 9]. While this may be true in some disease cases, a handful of plant deformations due to the influence of environmental factors such as nutrients deficiency exhibit similar discolorations as some diseases [1, 4, 11]. This will inevitably lead to missed ROI and ultimately, misclassification. Even the few methods that employed lesion localization [41], the criteria for subdivision of lesions were only loosely characterized and primarily based on superficiality. To the best of our knowledge, none segment categorically based on pathological analogy.

B. Early and late blight from a pathological point of view

The analogical pattern of EB disease symptom is very similar across the four common hosts (tomato, potato, pepper, and eggplant). They start with small dark brown or black necrotic spots or lesions which later enlarge forming concentric rings with a bulls-eye pattern surrounded by yellowish (symptomatic) zone [14, 15]. In the case of LB, initial infection symptoms start with small dark lesions often on leaf tips, after which it manifest to dark brown or black water-soaked lesions occasionally with a pale yellowish-green border that fades into the healthy tissue [16, 17]. Both diseases manifest by expanding over the healthy green tissue with a fuzzy zone in-between healthy tissue and disease lesion. Regarding this, each leaf would have four regions: leaf healthy tissue that is purely green, leaf symptomatic region (yellowish or green-whitish area), leaf necrotic region (brown or black area), and blurred region in-between healthy and disease lesion. However, it should be noted that the blurred region is not part of disease lesion [15]. It thus follows the characteristic in TABLE I.

TABLE I: DISEASE LESION CHARACTERISTICS FROM PATHOLOGICAL ANALOGY

Disease	***Disease lesion type***	***Pathological characteristics***
Early blight (EB)	Symptomatic	yellowish or yellowish-green zones
	Necrotic	dark brown or black necrotic (concentric) spot(s) or lesions
Late blight (LB)	Symptomatic	water-soaked (whitish) zones. Occasionally containing some yellowish part also
	Necrotic	dark-brown or black spot(s) or lesions

Majority of the presented works use texture as the main feature while others combine both texture and color features as presented in comprehensive reviews [1, 7, 8, 10, 22]. This is so because most diseases symptoms exhibit homogenous patterns such as discoloration along the leaf surface [2, 23], and extracting a limited number of locally optimized features that would easily discriminate between diseases is often trivial which in turn lead to the huge numbers. Many abiotic disorders have distinct visual symptoms that are leveraged to identify and classify them accurately. Few of these diseases such as early and late blight, however, peculiarly share those distinct features that not only affect the ability of machine learning algorithms in providing accurate results but human experts as well [7, 24]. The degree of similarity often also leads to tricky challenges such as resulting in intensive computations that often ended up yielding significant misclassification error.

Despite the number of successes, disease assessment through imagery analysis was found in most cases are not in close agreement to actual values [2, 11]. Bock *et al.* concluded that the vast majority of presented works often gave accurate results in some specific cases, but generally, time-consuming even when so [2]. A reason could be the fact that current image analysis does not offer a direct way of distinguishing actual symptoms localized into necrotic or symptomatic caused by pathogens. As the area of diseased tissue is divided into symptomatic and necrotic counted as a number of colonies [14, 25], allocating a number to disease lesion description allows the stage of disease development to be numerically assessed or estimated [2, 26, 27]. This advantage clearly describes the disease development stage and of immense importance to Raters for numerous interpretation such as in plant breeding programs [28] and yield loss estimation [29]. A critical review made by Hughes and Madden (1995) [30] and Madden and Hughes (1999) [26] reassessed the methodologies for the analysis of disease particularly concerning aggregated disease patterns such as spatial hierarchy and heterogeneity distribution pointing the potential for error in correlations between experiments and treatments if overlooked. As highlighted, it is great interest to identify novel markers that can reflect various plant phenotyping states ensuring high throughput through exploration of the relationship between temporal signatures and anatomy of plants [1, 31-33]. It is in this regard that this paper proposes a new automated machine vision pattern analysis-based phenotyping for localizing and quantifying early and late blight symptomatic and necrotic regions in vegetable plant leaves. The uniqueness of this approach is on using soft computing algorithms and the analogy of plant disease to segment local disease lesion colonies that will later be used to track pattern changes and produce dissimilarity features for simple characterization of the two diseases. As part of a complete plant disease detection system, it is also envisaged that the results would lead to new features for discriminating between and severity estimation of early and late blight vegetable diseases using soft computing methods. Furthermore, a novelty target of this work is to pioneer an intelligent blend of the human expert system concept into the computer vision and machine learning techniques.

II. MATERIALS AND METHODS

Considering the properties of both diseases, their similarity is most often considered as the basis for characterization by which features are tuned. However, a recent survey had described symptom similarity between distinct diseases as a major challenge in the application of machine learning even in well-trained models leading to a large portion of research focusing on only diseases with different symptoms [7, 34, 35]. This can be mainly featured to lack of essential consideration to the distinct, dissimilar patterns derived from the pathological analogy. It is in this regard that algorithm implementation and evaluation were performed based on early and late blight disease pathological anatomies, specifically, the homogeneous pattern of disease manifestation focusing on distinct dissimilarity. As part of a complete system, the experiments were divided into two phases. The 1st phase is where individual symptomatic (R_S), necrotic (R_N), and blurred (R_B, in-between healthy and

disease) regions were identified, segmented and quantified. Whereas in the 2nd phase, the objective is the extraction of the feature properties established in the first phase. However, this research paper focused on the former (i.e., the 1st phase).

A. Image dataset

The PlantVillage public image dataset [36] consisting of healthy and diseased (early and late blight) leaf images were utilized along with other images collected from the internet to compensate for pepper blight images. A detailed breakdown of image data is given in TABLE II. These data were chosen as the diseases highlighted peculiar disease anatomy factor where symptom pattern regions are not always palpable. Furthermore, early and late blight disease symptoms exhibit similar symptoms across the solanaceous vegetable crops [24, 37-39] including the three considered in this research, due to this they are most often difficult to characterize. The whole dataset was spilt, randomly for each class (late blight – LB, early blight – EB) into two groups as training and testing to allow for proper assessment of characterization features. All the images for the three classes are of the same scale size of 256×256.

B. Methodology

It has been established that pixels exhibiting higher deviations towards the green hue in comparison to blue and red are of healthy tissue [12]. The study also presented an automatically extended region of interest (EROI) segmentation to incorporate symptom progression information by extending the border region to cover fuzzy zones (blurred tissue) using color homogeneity thresholding. Part of that methodology is being used here.

1) 1. EROI segmentation

In this step, the already established EROI segmentation algorithm [12] is utilized. Pixels of the healthy green tissues are masked based on the computed ratio of green color to red and blue except for those within the computed extended region. On this basis, threshold values were set between four pixels groups to generate four masks and then combined to form the final segmentation mask leaving only the EROI [12].

2) 2. Segmentation of symptom lesion colonies

Seldom, the analogical pattern of EB disease symptom is found to be similar to that of LB. However, following closely EB necrotic spots or lesions form concentric rings having a bulls-eye pattern surrounded by yellowish (symptomatic) zone [14, 15]. Hence, as an extension of the EROI segmentation in [12] the target of this step is on identifying and localizing colonies that exhibit the three characteristics; symptomatic region (R_S) comprising of yellowish and water-soaked zones, necrotic (R_N) for dark brown or black regions, and blurred region (R_B , in-between healthy and symptomatic). The EROI represented as I_{EROI} is then a combination of the three such that:

$$I_{EROI}(x,y) = R_S(x,y) + R_N(x,y) + R_B(x,y) \quad (1)$$

To analyze diseased segments, the EROI image pixels are transformed from RGB to CIE L*a*b* and HSV color spaces [40]. The former decomposes the image into three channels as L^* for the lightness (darkest black at $L^* = 0$, and the brightest white at $L^* = 100$) and a^* and b^* for the green–red and blue-yellow color components. Scaling and limits of the a^* axes normally depend on the specific implementation [40], which in this case, the chromaticity to identify discoloration, thus selecting the range of ±128 (for 8-bit integer). The latter represents *H* as Hue resembles pure color described by a fraction between 0 and 1 that specifies the position of the corresponding pure color on the representative color wheel, *S* as Saturation representing how white the color is, and *V* Value also called its brightness describing how dark the color is [40]. Both were considered in this study as they were designed to be perceptually uniform concerning the way humans visually perceive color. Figure 2 depicts the L*a*b* and HSV color wheels.

The process starts by first obtaining individual representative threshold ranges for *H-channel* and *a-channel* as $low\ value \leq t_i < high\ value$ for each of the discoloration regions symptomatic, necrotic, and blur as $i = R_S, R_N, R_B$. The thresholds are applied to pixels in the two channels, thereby generating two binary masks such that:

$$m_1(R_i) = \begin{cases} 1 & t_{Htl} \leq P(x,y) \leq t_{Hth} \\ 0 & otherwise \end{cases} \quad (2)$$

$$m_2(R_i) = \begin{cases} 1 & t_{atl} \leq P(x,y) \leq t_{ath} \\ 0 & otherwise \end{cases} \quad (3)$$

Where $i = S, N, B$ represents symptomatic, necrotic, and blur, respectively, and $P(x,y)$ individual pixels. Then, the final mask for each region would be:

$$M(R_i) = m_1(R_i) + m_2(R_i) \quad (4)$$

Following the EB disease analogy, segmenting R_i pixels would be:

TABLE II. DISEASE LESION LOCALIZATION ACCORDING TO PATHOLOGICAL ANALOGY ON HOST SPECIE

Disease Lesion Type	*Symptom analogy*	*Vegetable specie*	*N0. of samples per specie*	*Sample image*	
				Original	*EROI*
Symptomatic	yellowish-green or water-soaked zones	Potato, tomato, and pepper	Potato = 500 Tomato = 500 Pepper = 30		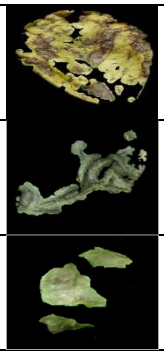
Necrotic	dark-brown or black zones				
Blur	Fuzzy zone (in between symptomatic/necrotic and healthy)				

$$P_S(x,y) = \{(x,y) \in I_{EROI} | \Phi_1(x,y)\} \quad (5)$$

$$P_N(x,y) = \{(x,y) \in I_{EROI} | \Phi_2(x,y)\} \quad (6)$$

Where $\Phi_2, \Phi_1 = M(R_S), M(R_S)$ and $P_S(x,y)$, $P_N(x,y)$ are symptomatic and necrotic pixel regions respectively. Blur region pixels would then be:

$$P_B(x,y) = I_{EROI}(x,y) - \{P_S(x,y) + P_N(x,y)\} \quad (7)$$

Equations (5), (6), and (7) are used to localize each disease lesion region (Fig. 1).

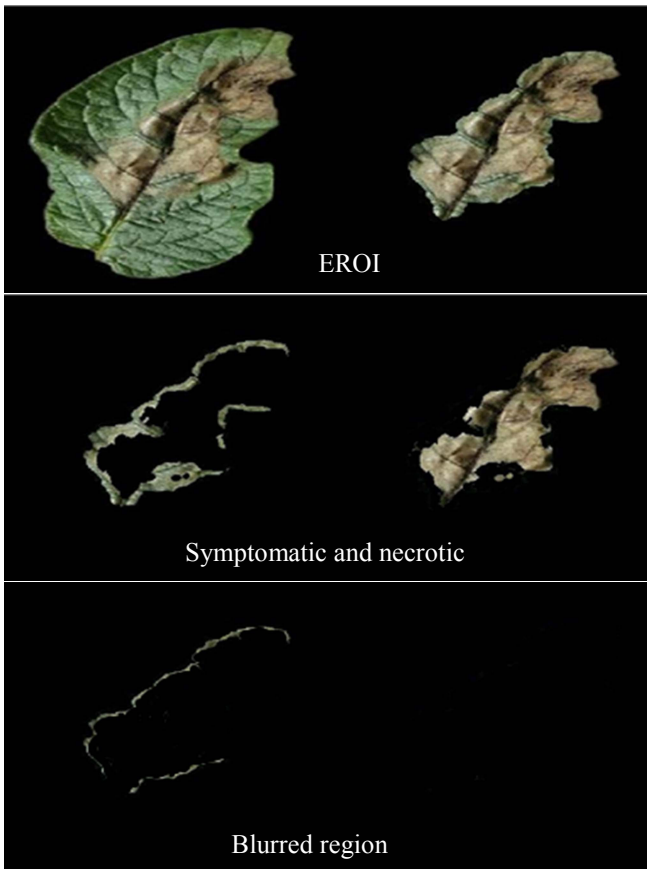

Fig. 1: Steps in the algorithm for localizing disease lesion colonies. The leaf sample is that of a potato infected with late blight.

3) Lesion quantization

For every segmented lesion colony, the area is measured as the total number of pixels it contains. Lesion quantization will not only help in accurately measuring disease severity but could aid in predicting the stage of disease development as well. Given the total number of leaf pixels in the original image as $I(x,y)$, then the total number of diseased pixels will be:

$$I_D(x,y) = I(x,y) - I_{EROI}(x,y) \quad (8)$$

Such that:

$$I_D(x,y) = \sum_{i=S,N,B} P_i(x,y) \quad (9)$$

C. Data analysis and Validation of the proposed algorithm

Despite the inability to ground-truth boundaries due to subjectivity, it is deemed important to obtain a measure of the algorithm's performance. Though removing subjectivity from such manual segmentation process is impossible [41], care was taken to reduce it to the barest minimum. Thus, the pixels of each of the lesion colonies were manually labeled and segmented by an expert.

All the data analysis was carried out using MATLAB R2017b (The MathWorks Inc., Natick, MA) program. Using the manual measurements as the ground truth, the following were calculated: the percentage of missed disease lesion pixels in each category (false negatives, FN and false positives, FP), and the percentage of missed blurred pixels (SB). The first two statistics represent the error in measurement, while the third statistic demonstrates the general behavior of the algorithms in dealing with the blurred regions. Also, a comparison was made with the results yielded by the proposed algorithm with two other segmentation methods that considered homogeneity.

The distribution of error N_e for each of the localized regions that indicates the magnitude of error expected in each case was calculated as N_d/N_T, where N_d is the number of pixels misclassified, and N_T is the total number of pixels in the leaf. The recall, also known as the true positive rate was computed as $TP/(TP + FN)$ where TP and FN are true positive and false negative rates. This also reflects the performance of the proposed algorithm in accurately classifying lesion pixels.

III. Results

TABLE III presents the segmentation performance of the proposed algorithm following the three disease lesion regions. The proposed algorithm was consistently more accurate when compared with the other two techniques: not only the error rates lower in all disease categories, but the proposed algorithm was the only method that was consistently robust quantifying disease lesion from the lesion colonies.

The results (TABLE III) show FP of the proposed method is lower (0.3% to 1.3%) in all lesion categories compared to Camargo's (1.2% to 1.5%) and is within close uniformity

TABLE III. Summary Of Segmentation Performance (in % of cases in each class) Of The Proposed Algorithm. *FP, FN*, Represent Missed Disease Lesion Pixels, *SB* Represent Missed Blurred Pixels, And NE Distribution Of Error

Result Summary	**Camargo and Smith [42]**				**Barbedo [41]**				**Proposed**			
Lesion Region	***FP***	***FN***	***SB***	N_e	***FP***	***FN***	***SB***	N_e	***FP***	***FN***	***SB***	N_e
Symptomatic	1.5	7.2	94.0	4.2	1.4	5.6	91.0	3.0	1.3	4.4	15.2	2.8
Necrotic	1.2	7.3	91.5	4.3	0.5	5.3	92.4	2.9	0.3	1.8	03.6	0.6

with Barbados (0.5% to 1.4%), though slightly higher. The proposed algorithm is more robust in characterizing symptomatic and necrotic regions from the blurred as indicated by FN (0.8% to 4.4%) compared to the other two (5.3% to 7.3%). The proposed algorithm also shows a significant decrease by no less than 80% in the proportion of pixels missed in the blurred region classified as symptomatic or necrotic (3.6% to 15.2%) compared to the other two algorithms (91.5% to 97.2%) and (60.1% to 92.4%). Though the ratio of the blurred region to disease lesion size is small ranging from 5% to 22%, its significance cannot be underrated considering it will provide vital information about the disease progression and severity.

The true positive rate (TP, TABLE IV) indicated the performance of the algorithm in accurately localizing the disease lesion pixels into symptomatic and necrotic regions. Having an average accuracy of 96.9%, the algorithm outperforms the other two, which stood at 92.8% and 94.6%.

TABLE IV. TRUE POSITIVE RATE (TP) OF THE PROPOSED ALGORITHM, COMPARING WITH TWO OTHER METHODS

Method	**Camargo and Smith**		**Barbedo**		**Proposed**	
Disease lesion region	***S***	***N***	***S***	***N***	***S***	***N***
TP	92.8%	92.7%	94.4%	94.7%	95.6%	98.2%

IV. DISCUSSION

The success of the proposed algorithm is partly featured to the EROI segmentation [12] as it accurately captures the border region between blurred and healthy tissue. However, two main sources of error were the most frequent causes of FPs and FNs. The first is due to their nature of not always having pronounced diseased border. The blurred region, particularly for late blight disease, often have several pixels that should have been included in either the healthy tissue or symptomatic region in the ground truth. This explains the slightly high proportion of pixels (15.2%) identified by the algorithm as symptomatic. Despite this nature, the algorithm was able to lower the error rate (N_e, 2.8% to 0.6%) as opposed to other existing methods (Camargo and Smith, 4.3% to 4.2%; and Barbados, 3.0% to 2.9%). The second error was in leaves with early stages of infection have characteristically small symptom units and are less pronounced, references (presumed actual values measured by the expert) may not be entirely accurate which in turn made those distortions a more prominent source of error. Another source of error was because of isolated outlier pixels that, despite being part of the symptomatic region, have characteristics more closely related to the fuzzy zone.

The overall performance of the proposed algorithm indicated great promise in having the complete hybrid automatic system for plant disease detection, incorporating intelligent expert analogy of diseases.

V. CONCLUSION

The main contribution of this paper is on using a combination of soft computing algorithms with expert pathological disease analogy to automatically identify, segment, and quantize local disease lesion colonies. Regarding this, the proposed algorithm is simple to implement, is based on the arithmetic manipulation and threshold application to the color channels designed to be perceptually uniform concerning the way humans visually perceive color. Compared with other existing works, the results indicate that the algorithm performs incredibly well outperforming the others in localizing symptomatic, necrotic, and blurred disease lesion regions. This substantiates the superiority of the proposed algorithm in localizing the three lesion colonies following the disease's analogies and as a pioneer of an intelligent blend of the human expert system concept into the computer vision and machine learning techniques.

As the first phase of a complete plant disease detection system, further studies are ongoing to track pattern changes and produce dissimilarity features for the simple characterization of the two diseases and to estimate their severity.

ACKNOWLEDGMENT

The authors thank the Ministry of Education Malaysia and Universiti Teknologi Malaysia (UTM) for their support under the University Grant (UTM Flagship). Grant number PY/2018/02995 under project title: Distorted Images Pre-processing for Deep Neural Network Classification.

REFERENCES

[1] K. Mochida *et al.*, "Computer vision-based phenotyping for improvement of plant productivity: a machine learning perspective," *GigaScience,* vol. 8, no. 1, p. giy153, 2018.

[2] C. Bock, G. Poole, P. Parker, and T. Gottwald, "Plant disease severity estimated visually, by digital photography and image analysis, and by hyperspectral imaging," *Critical Reviews in Plant Sciences,* vol. 29, no. 2, pp. 59-107, 2010.

[3] H. Nilsson, "Remote sensing and image processing for disease assessment," *Protection Ecology,* vol. 2, pp. 271-274, 1980.

[4] R. Blanchette, "New technique to measure tree defect using an image analyzer [Wood-destroying microorganisms]," *Plant Diseases,* 1982.

[5] S. Lindow, "Estimating disease severity of single plants," *Phytopathology,* vol. 73, no. 11, pp. 1576-1581, 1983.

[6] S. Lindow and R. Webb, "Quantification of foliar plant disease symptoms by microcomputer-digitized video image analysis," *Phytopathology,* vol. 73, no. 4, pp. 520-524, 1983.

[7] J. G. A. Barbedo, "A review on the main challenges in automatic plant disease identification based on visible range images," *Biosystems Engineering,* vol. 144, pp. 52-60, 2016.

[8] S. Kaur, S. Pandey, and S. Goel, "Plants Disease Identification and Classification Through Leaf Images: A Survey," *Archives of Computational Methods in Engineering,* journal article January 19, 2018.

[9] A. M. Mutka and R. S. Bart, "Image-based phenotyping of plant disease symptoms," *Frontiers in plant science,* vol. 5, p. 734, 2015.

[10] S. Sankaran, A. Mishra, R. Ehsani, and C. Davis, "A review of advanced techniques for detecting plant diseases," *Computers and Electronics in Agriculture,* vol. 72, no. 1, pp. 1-13, 2010/06/01/ 2010.

[11] T. U. Rehman, M. S. Mahmud, Y. K. Chang, J. Jin, and J. Shin, "Current and future applications of statistical machine learning algorithms for agricultural machine vision systems," *Computers and Electronics in Agriculture,* vol. 156, pp. 585-605, 2019/01/01/ 2019.

[12] A. M. Abdu, Mokji M.; Sheikh, U. U, "An Investigation into The Effect of Disease Symptoms Segmentation Boundary Limit on Classifier Performance in Application Of Machine Learning for Plant Disease Detection," *International Journal of Agricultural, Forestry & Plantation (ISSN No: 2462-1757)*

Journal vol. 7, no. 6, pp. 33 - 40, December 2018, Art. no. IJAFP_39.

[13] X. E. Pantazi, D. Moshou, and A. A. Tamouridou, "Automated leaf disease detection in different crop species through image features analysis and One Class Classifiers," *Computers and Electronics in Agriculture,* vol. 156, pp. 96-104, 2019/01/01/ 2019.

[14] R. Chaerani and R. E. Voorrips, "Tomato early blight (Alternaria solani): the pathogen, genetics, and breeding for resistance," *Journal of general plant pathology,* vol. 72, no. 6, pp. 335-347, 2006.

[15] R. D. Rands, *Early blight of potato and related plants*. Agricultural Experiment Station of the University of Wisconsin, 1917.

[16] W. E. Fry and S. B. Goodwin, "Re-emergence of potato and tomato late blight in the United States," *Plant Disease,* vol. 81, no. 12, pp. 1349-1357, 1997.

[17] M. Nowicki, E. U. Kozik, and M. R. Foolad, "Late blight of tomato," *Translational genomics for crop breeding,* vol. 1, pp. 241-265, 2013.

[18] J. F. Molina, R. Gil, C. Bojacá, F. Gómez, and H. Franco, "Automatic detection of early blight infection on tomato crops using a color based classification strategy," in *Image, Signal Processing and Artificial Vision (STSIVA), 2014 XIX Symposium on*, 2014, pp. 1-5: IEEE.

[19] A. Camargo and J. Smith, "Image pattern classification for the identification of disease causing agents in plants," *Computers and Electronics in Agriculture,* vol. 66, no. 2, pp. 121-125, 2009.

[20] D. Sena Jr, F. Pinto, D. Queiroz, and P. Viana, "Fall armyworm damaged maize plant identification using digital images," *Biosystems Engineering,* vol. 85, no. 4, pp. 449-454, 2003.

[21] S. Arivazhagan, R. N. Shebiah, S. Ananthi, and S. V. Varthini, "Detection of unhealthy region of plant leaves and classification of plant leaf diseases using texture features," *Agricultural Engineering International: CIGR Journal,* vol. 15, no. 1, pp. 211-217, 2013.

[22] F. Martinelli *et al.*, "Advanced methods of plant disease detection. A review," *Agronomy for Sustainable Development,* vol. 35, no. 1, pp. 1-25, 2015.

[23] P. S. Ojiambo, J. Yuen, F. van den Bosch, and L. V. Madden, "Epidemiology: Past, Present, and Future Impacts on Understanding Disease Dynamics and Improving Plant Disease Management—A Summary of Focus Issue Articles," *Phytopathology,* vol. 107, no. 10, pp. 1092-1094, 2017/10/01, 2017.

[24] L. Kenyon, S. Kumar, W.-S. Tsai, and J. d. A. Hughes, "Chapter Six - Virus Diseases of Peppers (Capsicum spp.) and Their Control," in *Advances in Virus Research*, vol. 90, G. Loebenstein and N. Katis, Eds.: Academic Press, 2014, pp. 297-354.

[25] M. Ridout and X.-M. Xu, "Relationships between several quadrat-based statistical measures used to characterize spatial aspects of disease incidence data," *Phytopathology,* vol. 90, no. 6, pp. 568-575, 2000.

[26] L. Madden and G. Hughes, "An effective sample size for predicting plant disease incidence in a spatial hierarchy," *Phytopathology,* vol. 89, no. 9, pp. 770-781, 1999.

[27] W. Turechek and L. Madden, "A generalized linear modeling approach for characterizing disease incidence in a spatial hierarchy," *Phytopathology,* vol. 93, no. 4, pp. 458-466, 2003.

[28] F. W. Nutter and P. D. Esker, "The role of psychophysics in phytopathology: The Weber–Fechner law revisited," *European Journal of Plant Pathology,* vol. 114, no. 2, pp. 199-213, 2006.

[29] E. C. Oerke, "Crop losses to pests," *The Journal of Agricultural Science,* vol. 144, no. 1, pp. 31-43, 2006.

[30] L. Madden and G. Hughes, "Plant disease incidence: distributions, heterogeneity, and temporal analysis," *Annual Review of Phytopathology,* vol. 33, no. 1, pp. 529-564, 1995.

[31] N. Shakoor, S. Lee, and T. C. Mockler, "High throughput phenotyping to accelerate crop breeding and monitoring of diseases in the field," *Current opinion in plant biology,* vol. 38, pp. 184-192, 2017.

[32] A. Singh, B. Ganapathysubramanian, A. K. Singh, and S. Sarkar, "Machine learning for high-throughput stress phenotyping in plants," *Trends in plant science,* vol. 21, no. 2, pp. 110-124, 2016.

[33] P. Pandey, Y. Ge, V. Stoerger, and J. C. Schnabel, "High throughput in vivo analysis of plant leaf chemical properties using hyperspectral imaging," *Frontiers in plant science,* vol. 8, p. 1348, 2017.

[34] S. S. Chouhan, U. P. Singh, and S. Jain, "Applications of Computer Vision in Plant Pathology: A Survey," *Archives of Computational Methods in Engineering,* pp. 1-22, 2019.

[35] J. G. Barbedo, "Factors influencing the use of deep learning for plant disease recognition," *Biosystems Engineering,* vol. 172, pp. 84-91, 2018.

[36] S. P. Mohanty, D. P. Hughes, and M. Salathé, "Using deep learning for image-based plant disease detection," *Frontiers in plant science,* vol. 7, p. 1419, 2016.

[37] W. L. Morris and M. A. Taylor, "The Solanaceous Vegetable Crops: Potato, Tomato, Pepper, and Eggplant A2 - Thomas, Brian," in *Encyclopedia of Applied Plant Sciences (Second Edition)*, B. G. Murray and D. J. Murphy, Eds. Oxford: Academic Press, 2017, pp. 55-58.

[38] V. Bergougnoux, "The history of tomato: From domestication to biopharming," *Biotechnology Advances,* vol. 32, no. 1, pp. 170-189, 2014/01/01/ 2014.

[39] P. Padmanabhan, A. Cheema, and G. Paliyath, "Solanaceous Fruits Including Tomato, Eggplant, and Peppers," in *Encyclopedia of Food and Health*Oxford: Academic Press, 2016, pp. 24-32.

[40] M. D. Fairchild, *Color appearance models*. John Wiley & Sons, 2013.

[41] J. G. A. Barbedo, "A new automatic method for disease symptom segmentation in digital photographs of plant leaves," *European journal of plant pathology,* vol. 147, no. 2, pp. 349-364, 2017.

[42] A. Camargo and J. Smith, "An image-processing based algorithm to automatically identify plant disease visual symptoms," *Biosystems Engineering,* vol. 102, no. 1, pp. 9-21, 2009